International Journal of Advanced Technology and Social Sciences (IJATSS)
Vol.4, No.10, 2026: 1335-1350

Pushover Response and Plastic Hinge Evolution of Steel SMRF with Panel Zone Representation

Indah Nur Afiah[1*], Mentari Septanya Sitorus[2], Nursafanah Dzakiyah Almakassari[3]
[1,2]Universitas Negeri Makassar
[3]Universitas Muhammadiyah Pare-Pare
Corresponding Author: Indah Nur Afiah; indahnurafiah@unm.ac.id

A R T I C L E I N F O

Keywords: Steel Special Moment-Resisting Frame, Panel Zone, Pushover Analysis, Plastic Hinge

Received : 5 August
Revised : 23 September
Accepted: 23 October

©2026 Afiah, Sitorus, Almakassari: This is an open-access article distributed under the terms of the Creative Commons Atribusi 4.0 Internasional.

A B S T R A C T

This study investigates the pushover response and plastic hinge evolution of a six-story steel Special Moment-Resisting Frame (SMRF) incorporating panel zone representation. Nonlinear static pushover analyses were conducted in the X and Y directions using ETABS under displacement control, considering P–Delta effects. The structural response was evaluated through capacity curves, plastic hinge status and distribution, and interstory displacement. The maximum base shear reached 20,830.91 kN in the X direction at a roof displacement of 0.326 m, compared with 6,748.74 kN in the Y direction at 0.323 m. At the final reported analysis steps, 102 hinge records classified as Immediate Occupancy–Life Safety (IO–LS) were distributed across Stories 2–4 in the X direction, whereas 54 records were concentrated on Story 2 in the Y direction. The maximum recorded interstory displacements were 0.021915 m at Story 3 in the X direction and 0.040266 m at Story 2 in the Y direction. These findings demonstrate directional differences in lateral capacity, hinge-status distribution, and deformation response. Further assessment requires drift-ratio verification and comparison at equivalent roof displacements

INTRODUCTION

Special moment-resisting steel frames (SMRFs) are structural systems designed to resist lateral loads through the flexural action of structural members and their capacity for inelastic deformation. As lateral loads increase, the structural response can evolve from elastic to inelastic behavior, characterized by the formation of plastic hinges in structural members. The location and sequence of plastic hinge formation are critical for understanding plasticity distribution and structural response during seismic loading (Damcı et al., 2024; Estakhri & Nikkhoo, 2025). Siahaan and Prabowo (2026) showed that variations in plastic-hinge placement and modeling in steel frame systems can affect the plasticization mechanism and the structure's performance. Meanwhile, Pratiwi et al. (2026) examined plastic-hinge distribution in multi-story buildings through nonlinear analysis with varying shear-wall configurations.

One component that influences beam–column connection behavior in steel frames is the panel zone—the region of the column shaft surrounding the connection that undergoes shear deformation as forces and moments transfer. The representation of the inelastic behavior of the panel zone can affect the distribution of deformation and seismic demands on steel frames (Safaei et al., 2022; Skiadopoulos & Lignos, 2022). Therefore, modeling this component must be considered in the nonlinear response evaluation of steel structures.

Previous research by Afiah and Sitorus (2026) evaluated the seismic response of a six-story SMRF steel structure with panel zone modeling using spectral response analysis. Nonlinear static pushover analysis provided additional information on changes in structural capacity and the development of inelastic response as lateral displacement increases. This approach allows examination of the relationship between base shear and roof displacement, along with the development and distribution of plastic hinges (Applied Technology Council [ATC], 1996; Federal Emergency Management Agency [FEMA], 2005).

Based on this, this study aims to evaluate the pushover response and plastic hinge development in a six-story SMRF steel structure represented by a panel zone. The analysis was performed in the X and Y directions using ETABS to evaluate capacity curves, plastic hinge distribution, and displacement and inter-story deflection responses. The results are expected to provide insight into the nonlinear response characteristics of the structural model under investigation.

LITERATURE REVIEW

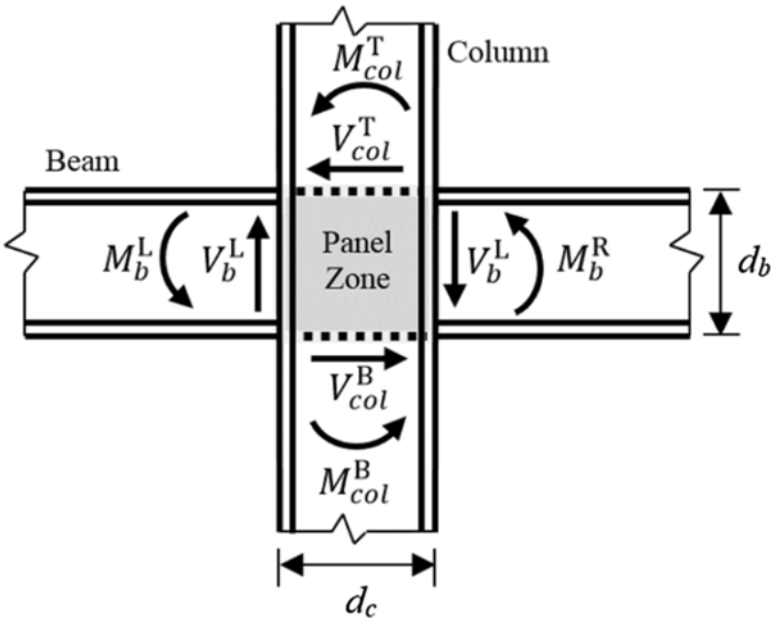
Nonlinear Analysis in Structural Performance Evaluation

Nonlinear analysis is used to evaluate a structure's response when its behavior exceeds elastic conditions. Two commonly used approaches are nonlinear static pushover analysis and nonlinear time-history analysis. Pushover analysis gradually increases lateral loads or displacements to obtain a capacity curve and observe the development of inelastic behavior. In contrast, time-history analysis calculates the structural response to a time-dependent seismic acceleration history. These two approaches serve different objectives and produce different outputs in seismic evaluation (ATC, 1996; FEMA, 2000, 2005).

Afiah et al. (2022) applied pushover analysis to evaluate the performance of reinforced concrete buildings based on ATC-40, FEMA 356, and FEMA 440. Meanwhile, Afiah et al. (2025) evaluated the response of reinforced concrete buildings in Palu using nonlinear time-history analysis with seven earthquake records. Both studies provide examples of applying nonlinear approaches to structural response evaluation, although the objects under study differ from those in this research. For steel structures, Siahaan and Prabowo (2026) also used pushover analysis to examine how variations in plastic-hinge modeling affect the global response and plasticization mechanisms in an inverted-V-type braced steel frame system. This study focuses on a six-story SMRF steel structure with panel zone representation and uses pushover analysis to examine capacity curves, plastic hinge development, and deformation response.

Panel Zone Modeling in Steel Moment-Resisting Frame Structures

The panel zone is the column web region surrounding the beam–column connection that undergoes shear deformation as forces and moments transfer (Ramadhan, 2021). This region's response can contribute to connection deformation and the overall behavior of the steel frame. Safaei et al. (2022) discuss modeling methods for beams, columns, and panel zones that account for force interaction, degradation, and plasticity distribution. Meanwhile, Skiadopoulos and Lignos (2022) evaluated the seismic requirements of moment-resisting steel frames by considering inelastic deformation in the panel zone. Both studies underscore the relevance of modeling connection components in the nonlinear analysis of steel frames.



Picture 1. Moment and shear forces occurring at the beam-column connection (Ramadhan, 2021)

Afiah and Sitorus (2026) previously evaluated the seismic response of a six-story SMRF steel model with panel-zone representation using spectral response analysis. This study employs nonlinear static pushover analysis to observe changes in capacity and the development of plastic hinges throughout

the loading stages. These approaches allow examination of structural response from different perspectives: response based on the earthquake spectrum and the development of inelastic behavior due to increased lateral displacement (ATC, 1996; FEMA, 2005).

Development of Plastic Hinges in Pushover Analysis

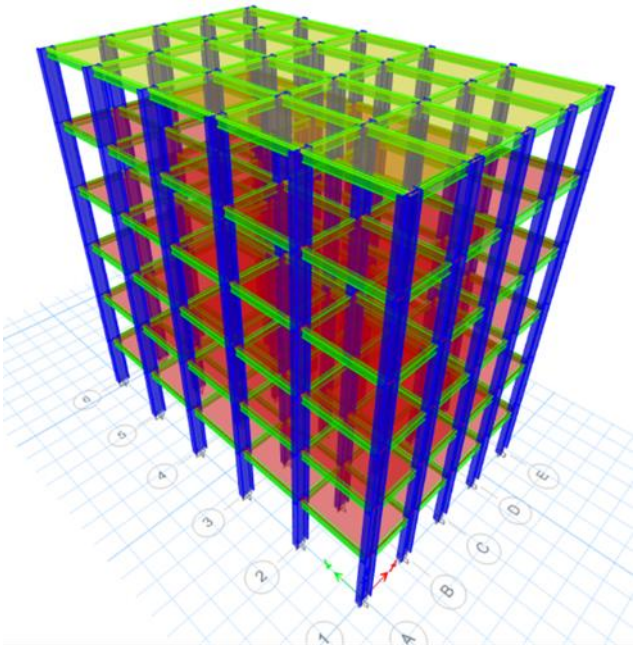
Plastic hinge represent local inelastic behavior in structural members when force or deformation demands exceed elastic limits. In SMRF steel structures, plastic hinge formation can identify where plasticization occurs and the sequence of changes in member behavior during loading. Capacity curves describe the structure's global response, while the status and distribution of plastic hinges provide information on the development of inelastic behavior at the element level (Damcı et al., 2024; FEMA, 2000, 2005).

Estakhri and Nikkhoo (2025) examined plastic hinge formation patterns in steel frames under near-field and far-field earthquakes using nonlinear time-history analysis. Damcı et al. (2024) developed a plastic hinge analysis method to determine pushover curves for three-dimensional frame structures. Additionally, Leiva Fuentes et al. (2024) examined plastic-hinge modeling in steel beams, considering local buckling as well as stiffness and strength degradation. Siahaan and Prabowo (2026) found that changes in plastic-hinge modeling in braced steel frame systems have limited effects on some global parameters but can influence the plastic-hinge mechanism and resulting performance level. Pratiwi et al. (2026) also evaluated plastic hinge distribution in multi-story buildings with different shear wall configurations using pushover analysis and nonlinear time-history analysis. These studies support the importance of evaluating plastic hinge development to understand the inelastic response of steel frames, despite differences in analytical methods and modeling focus.

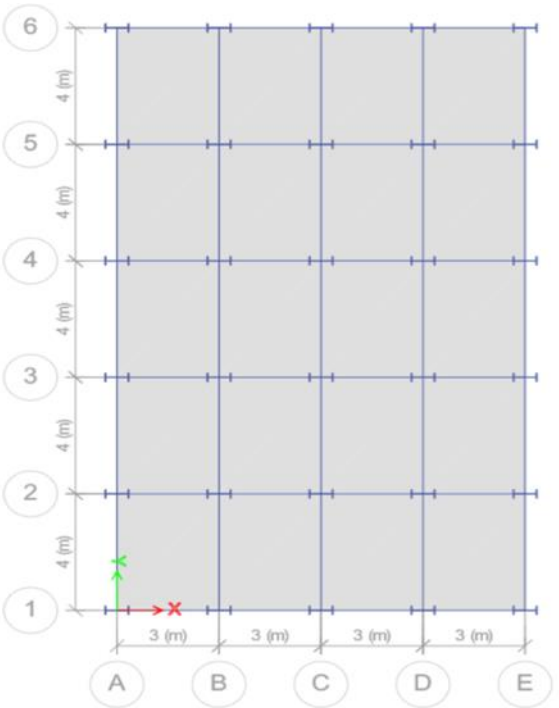
Based on this literature, this study focuses on the pushover response and plastic hinge development in a six-story SMRF steel structure using a zone-panel representation. Analyses were conducted in the X and Y directions by evaluating capacity curves, state changes, and the distribution of plastic hinges, as well as inter-story displacement and deflection responses.

METHODOLOGY

This study uses a six-story steel Special Moment-Resisting Frame (SMRF) model developed in ETABS. The model is based on Afiah and Sitorus (2026), with panel zones represented at the beam–column connections. The existing model was used to evaluate the nonlinear structural response without rebuilding the structure from scratch. Before analysis, the model was checked to ensure the material properties, element cross-sections, support conditions, loading, and analysis parameters were properly defined. P–Delta effects were also considered to account for second-order effects on the structural response.



Pic. 1



Picture 2. Modeling of the SMRF steel structure in the ETABS application: (Afiah & Sitorus, 2026)

The inelastic behavior of the structural elements was represented by assigning plastic hinges to beam and column elements in ETABS in accordance with ASCE/SEI 41-23 (American Society of Civil Engineers [ASCE], 2023). Beam hinges were defined based on the flexural moment about the local 3-axis (M3), whereas column hinges were defined using the combined axial force and biaxial bending interaction (P–M2–M3). The program output provided the plastic hinge status at each analysis step based on the assigned hinge properties.

Nonlinear static pushover analyses were performed separately in the X and Y directions using displacement control. Each analysis began with the gravity loading case (GRAVITY), followed by incremental increases in lateral displacement until the selected analysis displacement limit was reached or the analysis could no longer proceed. The roof displacement limit was set at 0.42 m, corresponding to 2% of the total structural height of 21 m. This value was adopted as the analysis limit for this study and was not a displacement target directly prescribed by ASCE/SEI 41-23 or SNI 1726:2019.

The structural response was evaluated using capacity curves, plastic hinge development, and deformation responses in both loading directions. Capacity curves were obtained from the relationship between base shear and roof displacement at each analysis step to identify the maximum recorded base shear and changes in global structural response. Plastic hinge development was examined through changes in hinge status and distribution across beam and column elements throughout the analysis. Roof displacement and story drift were also evaluated to characterize the distribution of deformation along the building height. These outputs were considered together to describe the nonlinear response of the structural model.

RESULTS

Pushover Capacity Curves

Pushover analysis was performed in the X and Y directions to determine the relationship between roof displacement and base shear in a Special Moment-Resisting Frame (SMRF) steel structure modeled as a panel zone. The analysis results consist of pairs of base shear and roof displacement data for each analysis step. These data were used to plot pushover capacity curves for each loading direction.

Table 1. Base Shear and Roof Displacement in the X Direction

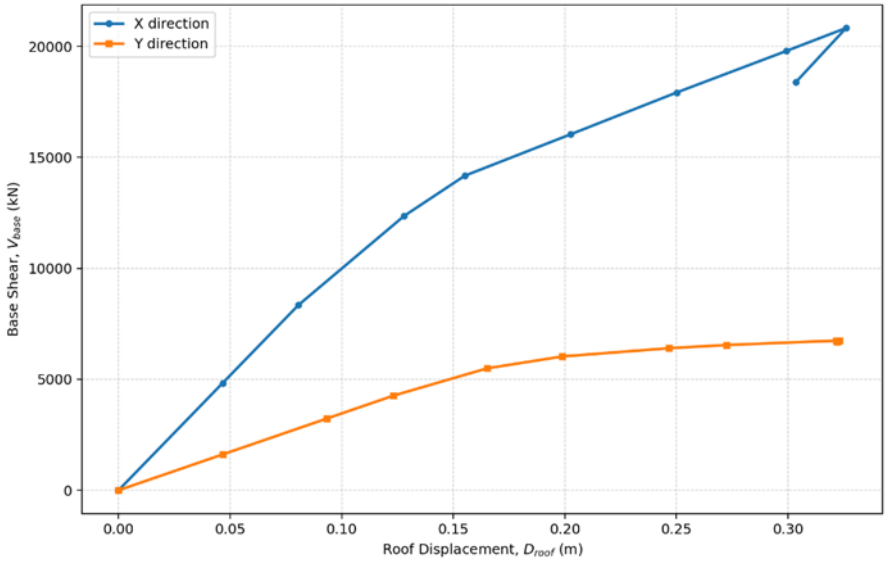
Analysis Step	Roof Displacement, D_{roof} (m)	Base Shear, V_{base} (kN)
0	0.000000	0.00
1	0.046667	4830.62
2	0.080633	8346.54
3	0.127942	12358.67
4	0.155143	14173.14
5	0.202554	16039.20
6	0.250052	17922.84
7	0.299366	19799.49
8	0.326027	20830.91
9	0.303619	18403.63

Table 2. Base Shear and Roof Displacement in the Y Direction

Analysis Step	Roof Displacement, D_{roof} (m)	Base Shear, V_{base} (kN)
0	0.000000	0.00

1	0.046667	1615.94
2	0.093333	3231.87
3	0.123063	4261.31
4	0.165139	5495.09
5	0.198892	6031.05
6	0.246696	6403.14
7	0.272483	6547.39
8	0.321566	6742.37
9	0.322961	6748.74
10	0.322961	6748.74
11	0.322068	6686.98

Based on these data, the pushover capacity curves for the X and Y directions are presented in Picture 3.



Picture 3. Pushover Capacity Curve in the X and Y Directions

In the X direction, the maximum base shear was recorded at 20,830.91 kN at a roof displacement of approximately 0.326 m. After reaching this maximum, the base shear at the final available analysis step was 18,403.63 kN. In the Y direction, the maximum base shear reached 6,748.74 kN at a roof displacement of approximately 0.323 m. In the final step, the base shear was recorded at 6,686.98 kN. Thus, both loading directions exhibit maximum base shear values within a relatively close range of roof displacements, although the recorded magnitudes of the base shear differ.

Plastic Hinge Evolution

The evolution of plastic hinge status was evaluated at each analysis step to examine the progression of inelastic response in the six-story steel Special Moment-Resisting Frame (SMRF) with panel zone representation. The ETABS output contained 948 hinge records at each analysis step. The hinge records were classified into the performance-status categories A–IO and IO–LS in both loading directions.

In the X direction, no hinge records were classified as IO–LS during Steps 0–4. The number increased to two records at Step 5, to 60 records at Step 6, and to 102 records at Step 7. This number remained unchanged through Step 9, the final reported analysis step. In the Y direction, no IO–LS records were identified during Steps 0–5. The number increased to three records at Step 6 and 30 records at Step 7, reaching 54 records at Step 8. The count remained unchanged through Step 11, the final reported analysis step.

Table 3. Evolution of Hinge Status in the X Direction

Analysis Step	A-IO	IO-LS	Total
0	948	0	948
1	948	0	948
2	948	0	948
3	948	0	948
4	948	0	948
5	946	2	948
6	888	60	948
7	846	102	948
8	846	102	948
9	846	102	948

Table 4. Evolution of Hinge Status in the Y Direction

Analysis Step	A-IO	IO-LS	Total
0	948	0	948
1	948	0	948
2	948	0	948
3	948	0	948
4	948	0	948
5	948	0	948
6	945	3	948
7	918	30	948
8	894	54	948
9	894	54	948
10	894	54	948
11	894	54	948

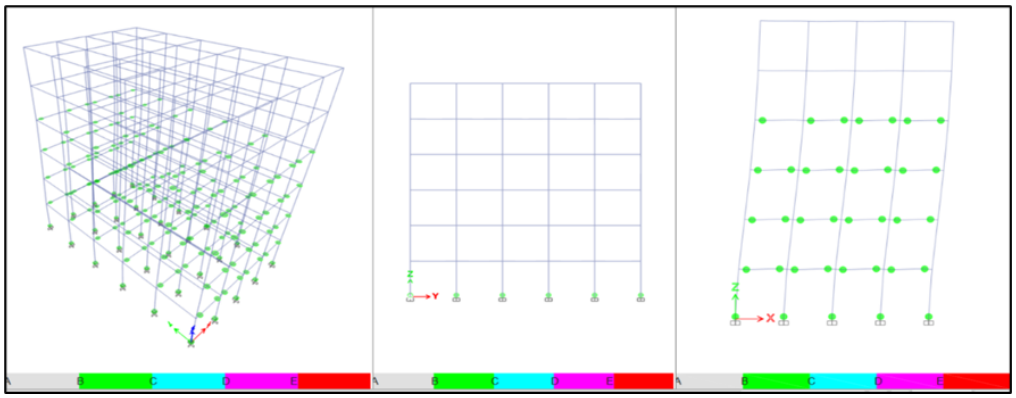
The distribution of IO–LS hinge records by story at the final reported analysis step is presented in Table 5.

Table 5. Distribution of IO–LS Hinge Records by Story

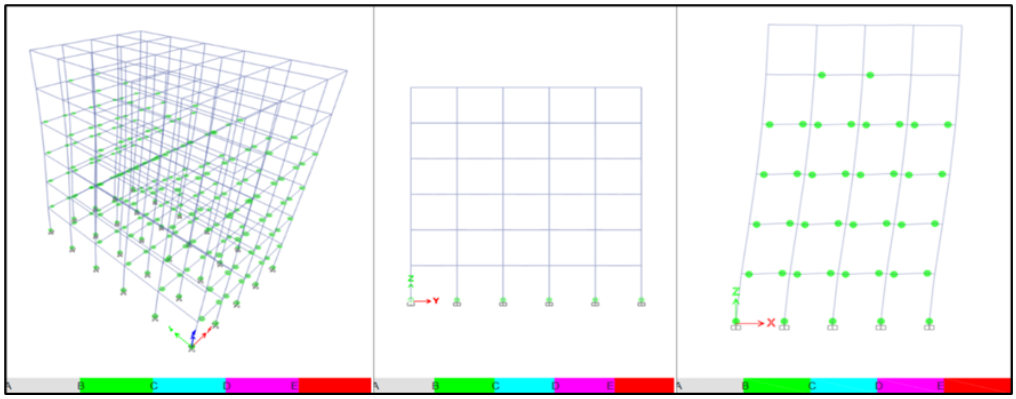
Story	X direction	Y direction
2	54	54
3	24	0
4	24	0
Total	102	54

In the X direction, the 102 IO–LS records were distributed across Stories 2, 3, and 4, with 54, 24, and 24 records, respectively. In contrast, all 54 IO–LS records in the Y direction were located on Story 2. These results indicate differences in hinge-status record distribution between the two loading directions.

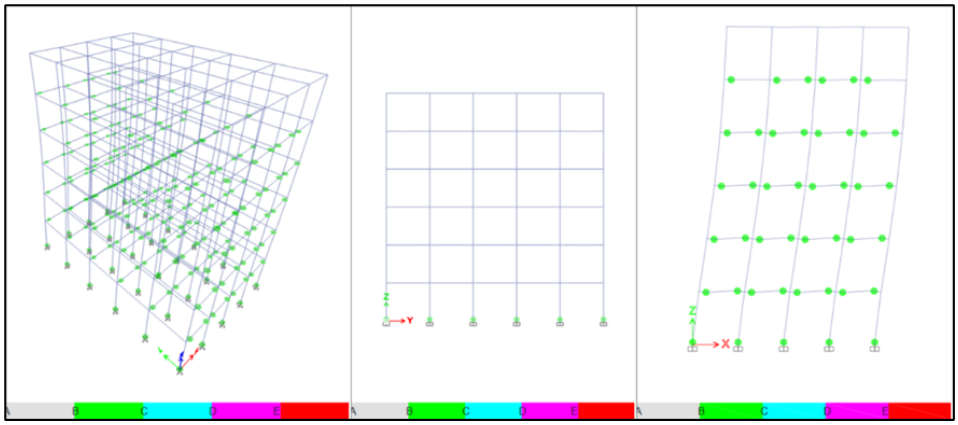
The separate Hinge State output showed 678 records classified as A–B, 266 as B–C, and four as D–E at Step 9 in the X direction. At Step 11 in the Y direction, 743 records were classified as A–B, 202 as B–C, and three as C–D. These hinge-state classifications are distinct from the performance-status categories reported in Tables 3–5.



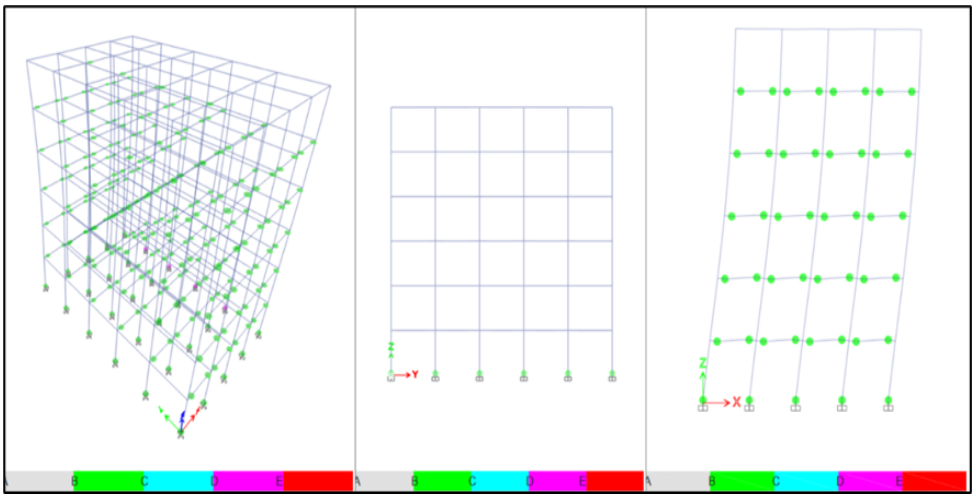
(a)



(b)

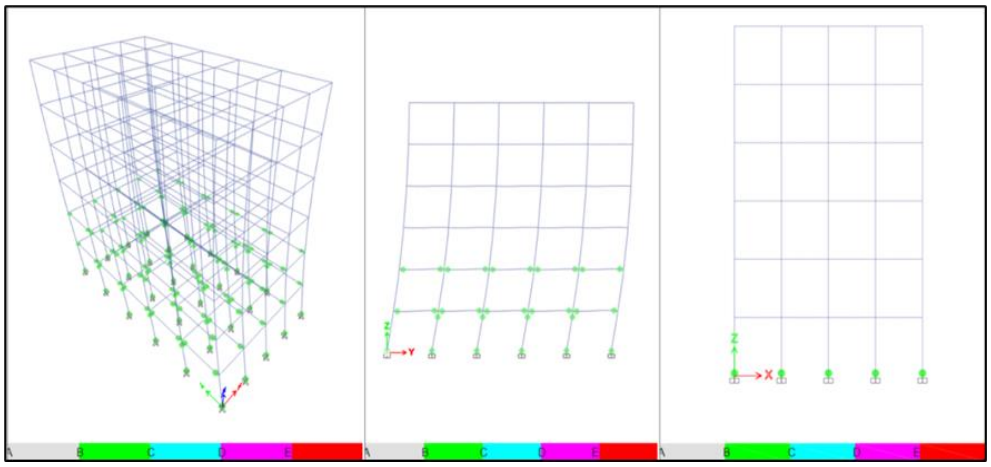


(c)

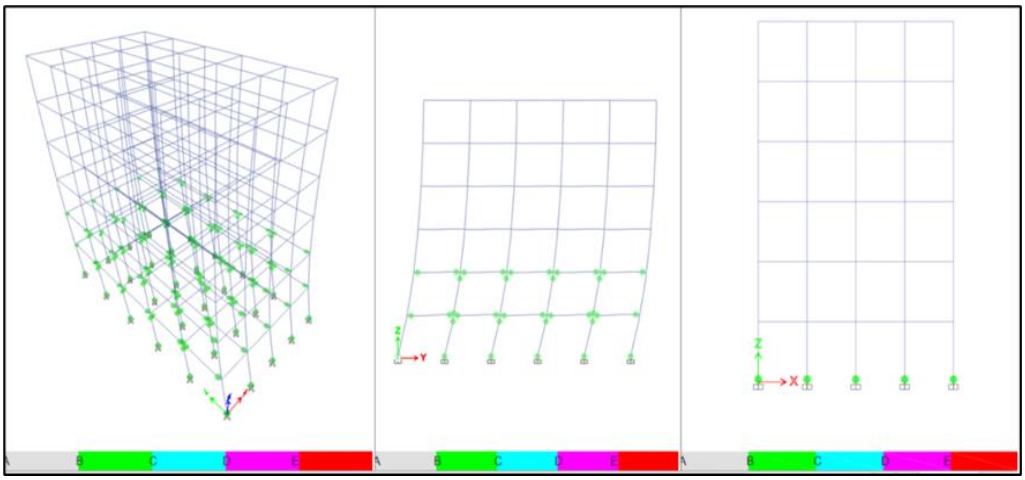


(d)

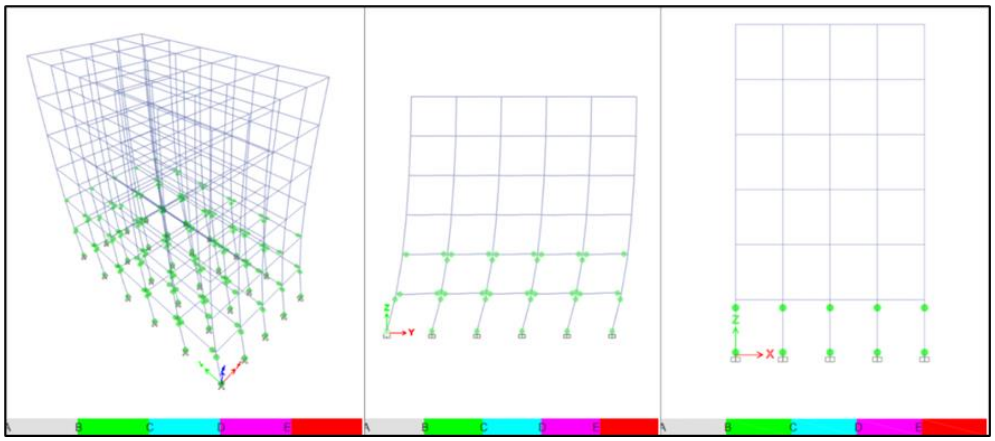
Picture 4. Plastic Hinge Distribution at Selected Steps in the X Direction (a) Step 4, (b) Step 5, (c) Step 6, (d) Step 9



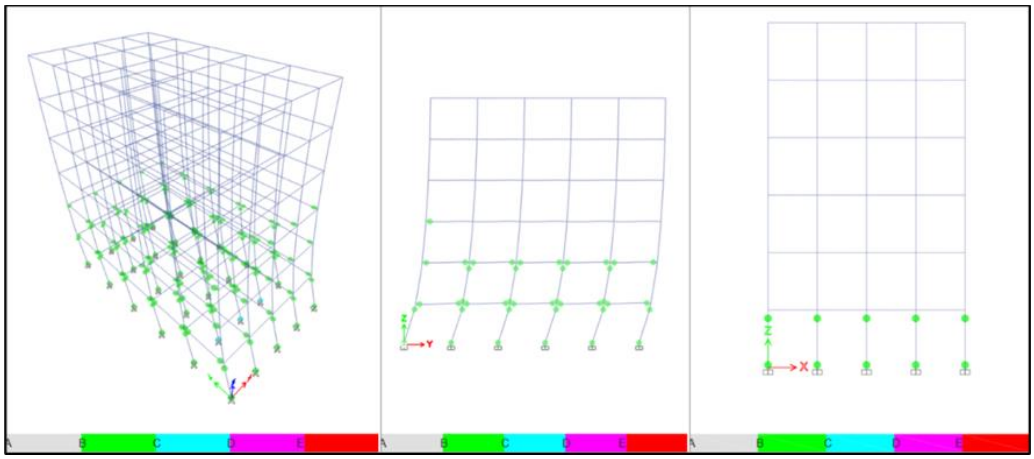
(a)



(b)



(c)



(d)

Picture 5. Plastic Hinge Distribution at Selected Steps in the X Direction
(a) Step 5, (b) Step 6, (c) Step 7, (d) Step 11

Story Drift Response

The story drift response was evaluated at each pushover analysis step to examine the distribution and evolution of interstory displacement along the building height. The ETABS output provided drift values for six story levels, from Story 2 to the roof level, in both loading directions. The complete results for the X and Y directions are presented in Tables 6 and 7.

Table 6. Story Drift at Each Analysis Step in the X Direction (m)

Step	Story 2	Story 3	Story 4	Story 5	Story 6	Roof
0	0.000001	0.000001	0.000002	0.000002	0.000002	0.000001
1	0.001807	0.003043	0.003003	0.002471	0.001795	0.001206
2	0.003123	0.005260	0.005190	0.004270	0.003103	0.002084
3	0.004904	0.008480	0.008428	0.006775	0.004786	0.003174
4	0.006071	0.010288	0.010227	0.008223	0.005749	0.003760
5	0.009816	0.013581	0.012848	0.010151	0.006980	0.004489
6	0.013418	0.016816	0.015469	0.012124	0.008304	0.005304
7	0.017156	0.020132	0.018146	0.014159	0.009725	0.006207
8	0.019140	0.021915	0.019598	0.015271	0.010509	0.006709

9	0.018403	0.020458	0.018119	0.014042	0.009613	0.006106

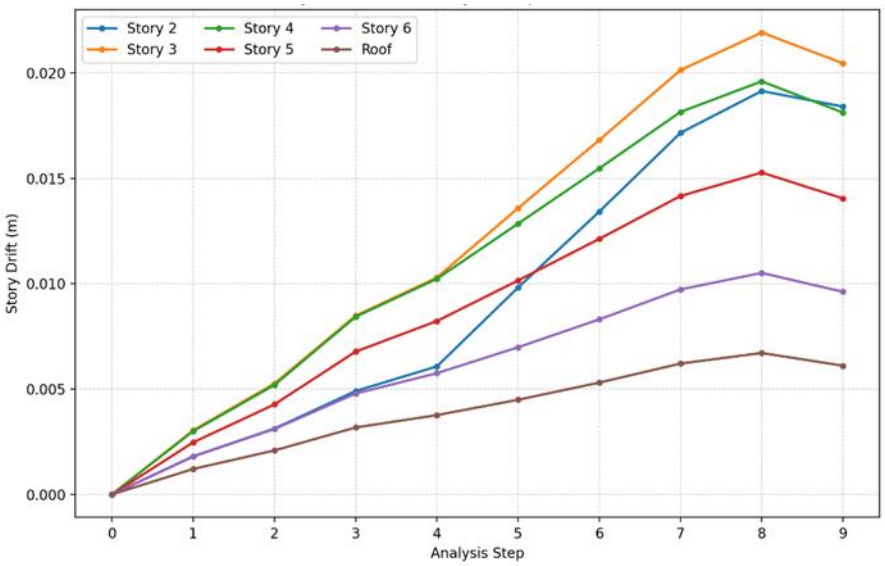
Table 7. Story Drift at Each Analysis Step in the Y Direction (m)

Step	Story 2	Story 3	Story 4	Story 5	Story 6	Roof
0	0.000003	0.000005	0.000005	0.000005	0.000005	0.000004
1	0.003061	0.003520	0.002824	0.002051	0.001279	0.000570
2	0.006126	0.007045	0.005654	0.004107	0.002563	0.001143
3	0.008078	0.009291	0.007457	0.005418	0.003381	0.001509
4	0.011731	0.012443	0.009681	0.006992	0.004361	0.001946
5	0.016530	0.014821	0.010834	0.007688	0.004789	0.002136
6	0.024696	0.018387	0.011835	0.008184	0.005088	0.002269
7	0.029258	0.020375	0.012285	0.008378	0.005206	0.002322
8	0.039855	0.022718	0.012877	0.008643	0.005364	0.002392
9	0.040145	0.022790	0.012897	0.008651	0.005369	0.002394
10	0.040145	0.022790	0.012897	0.008651	0.005369	0.002394
11	0.040266	0.022671	0.012789	0.008573	0.005320	0.002372

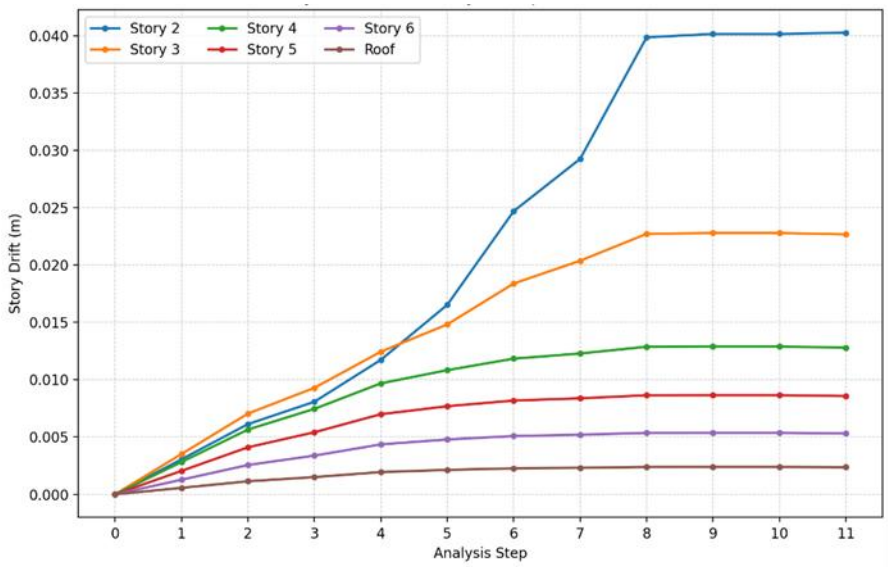
The results indicate that the distribution of story drift varied with the loading direction and analysis step. In the X direction, the maximum recorded story drift was 0.021915 m at Story 3 in Step 8. The values decreased slightly in Step 9, with the maximum recorded value reaching 0.020458 m at Story 3.

In the Y direction, the maximum recorded story drift was 0.040266 m at Story 2 in Step 11. The location of the maximum shifted from Story 3 during the initial analysis steps to Story 2 beginning in Step 5. The drift at Story 2 increased substantially in the later steps, while the values at the upper stories remained comparatively lower.

The corresponding drift distributions are illustrated in Pictures 6 and 7 for the X and Y directions, respectively.



Picture 6. Story Drift at Each Analysis Step in the X Direction



Picture 7. Story Drift at Each Analysis Step in the Y Direction

DISCUSSION

The results of the pushover analysis show differences in the structure's lateral response in the X and Y directions. The maximum base shear force in the X direction reached 20,830.91 kN, or approximately 3.09 times the maximum value in the Y direction of 6,748.74 kN. Both maximum values occurred at similar roof displacements: approximately 0.326 m in the X-direction and 0.323 m in the Y-direction. However, a comparison of maximum values does not fully capture the difference in capacity at equivalent deformation levels. A comparison of base shear forces at the same roof displacement is necessary to evaluate the difference in response between the two directions more directly.

Differences in loading directions are also evident in the distribution of IO–LS joint records. In the final step, the X-direction had 102 records spread across floors 2, 3, and 4, while the Y-direction had 54 records, all on floor 2. These results indicate that IO–LS joint records are more dispersed in the X direction, while in the Y direction they are more concentrated on a single floor. However, differences in the number and distribution of these records cannot directly determine which direction performs better. The evaluation must consider element location and type, joint acceptance criteria, and the contribution of deformation in beams, columns, and zone panels.

The story drift distribution reveals differences in the location of maximum responses. In the X-direction, the maximum story drift of 0.021915 m was recorded on the 3rd floor, whereas in the Y-direction, the maximum value of 0.040266 m was recorded on the 2nd floor. Thus, the maximum relative inter-story displacement recorded in the Y-direction is greater than that in the X-direction. However, values in meters alone are insufficient to assess compliance with allowable drift limits. Such an assessment requires the interstory drift ratio, obtained by dividing the relative inter-story drift by the corresponding story height, and then comparing it to the applicable limit. The concentration of joint records and maximum drift on the 2nd floor in the Y-direction indicates a

location that requires further review, but it is not sufficient to confirm the occurrence of a soft-story mechanism.

In both directions, the base shear force decreases after reaching the maximum recorded value. This decrease indicates a change in force response in the next analysis step, but does not in itself prove structural collapse. An examination of the convergence history, the joint status of individual elements, and the deformation capacity of components is required before a collapse mechanism can be established. Furthermore, the maximum roof displacement recorded in both directions remains below the selected analysis displacement limit of 0.42 m. Therefore, the available results describe only the response within the displacement range achieved.

Overall, the capacity curves, plastic hinge distribution, and story drift indicate that the structure's nonlinear response varies by loading direction. However, determining the seismic performance level requires an integrated evaluation of capacity, deformation, hinge acceptance criteria, and inter-story response. Comparing results at the same roof displacement and verifying the drift ratio will strengthen the interpretation of differences in the X- and Y-directional responses.

CONCLUSIONS AND RECOMMENDATIONS

Based on the pushover analysis of the SMRF steel structure using a zone-panel representation, the following conclusions were drawn.

1. Differences in capacity between the X and Y directions. The maximum base shear force in the X direction reached 20,830.91 kN at a roof displacement of approximately 0.326 m, while in the Y direction it reached 6,748.74 kN at a displacement of approximately 0.323 m. The maximum value in the X-direction is approximately 3.09 times that in the Y-direction. A comparison at the same roof displacement is still needed to more directly evaluate the difference in response between the two directions.
2. Distribution of plastic hinges. In the final step, 102 joint records with IO–LS status were found in the X direction, distributed across floors 2, 3, and 4, while 54 records were found in the Y direction, all located on floor 2. These results indicate a difference in the distribution pattern of joint records with IO–LS status between the two loading directions.
3. Story drift response. The maximum story drift value recorded in the X direction was 0.021915 m on the 3rd floor, while in the Y direction it was 0.040266 m on the 2nd floor. These values represent relative inter-story displacement in meters and cannot yet be used directly to determine compliance with allowable displacement limits.
4. Recommendations. Further evaluation should include comparing base shear forces at the same roof displacement, verifying the interstory drift ratio, examining joint locations on individual elements, and reviewing the analysis convergence history. These checks strengthen the seismic performance assessment and prevent conclusions about collapse mechanisms that are not yet supported by sufficient evidence.

FURTHER STUDY

This study examines the pushover response and plastic hinge development in a Special Moment-Resisting Frame (SMRF) steel structure modeled using a panel-zone representation. The analysis results indicate differences between the X and Y directions in lateral force capacity, plastic hinge distribution, and story drift. However, a more in-depth evaluation is needed to fully understand these behavioral differences.

Future research should compare base shear forces at the same roof displacement and evaluate the interstory drift ratio on each floor. Additionally, an examination of the location, element type, and sequence of plastic hinge development in beams, columns, and zone panels is necessary to identify patterns of inelastic response and potential inter-story deformation concentrations. A parametric analysis varying the zone panels' stiffness could also be conducted to evaluate its effect on lateral capacity and plastic hinge development.

Furthermore, nonlinear time-history analysis using multiple earthquake records can be performed to evaluate the structure's response to dynamic loading. This approach is expected to complement the pushover results and provide a more comprehensive understanding of the inelastic behavior of SMRF steel structures with panel-zone modeling.

REFERENCES

Afiah, I. N., & Sitorus, M. S. (2026). Seismic response of mid-rise steel SMRF with panel zone modeling. International Journal of Applied and Advanced Multidisciplinary Research, 4(5), 283–300. https://doi.org/10.59890/ijaamr.v4i5.218

Afiah, I. N., Ashad, H., & Rahman, M. J. (2022). Evaluasi kinerja struktur beton bertulang dengan pushover analysis berdasarkan ATC-40, FEMA 356 dan FEMA 440. Jurnal Flyover, 2(2), 99–110. https://doi.org/10.52103/jfo.v2i2.1347

Afiah, I. N., Rahman, M. J., Sitorus, M. S., & Ibrahim, Z. (2025). Structural response of a reinforced concrete building to earthquake excitation: A nonlinear time-history analysis case study in Palu, Indonesia. Journal of Civil Engineering, 40(3), 273–282. https://doi.org/10.12962/j20861206.v40i3.9318

American Society of Civil Engineers. (2023). Seismic evaluation and retrofit of existing buildings (ASCE/SEI 41-23). https://doi.org/10.1061/9780784416112

Applied Technology Council. (1996). Seismic evaluation and retrofit of concrete buildings (ATC-40). California Seismic Safety Commission.

Badan Standardisasi Nasional. (2019). SNI 1726:2019: Tata cara perencanaan ketahanan gempa untuk struktur bangunan gedung dan nongedung. Badan Standardisasi Nasional.

Badan Standardisasi Nasional. (2020). SNI 7860:2020: Ketentuan seismik untuk bangunan gedung baja struktural. Badan Standardisasi Nasional.

Damcı, E., Öztorun, N. K., & Çelik, T. (2024). A plastic hinge method for static pushover analysis of 3D frame structures. Australian Journal of

Structural Engineering, 25(4), 370–391. https://doi.org/10.1080/13287982.2024.2323865

Estakhri, M., & Nikkhoo, A. (2025). Investigating the pattern of plastic hinge formation in steel moment frames under near-field and far-field earthquakes. Discover Civil Engineering, 2, Article 227. https://doi.org/10.1007/s44290-025-00375-w

Federal Emergency Management Agency. (2000). Prestandard and commentary for the seismic rehabilitation of buildings (FEMA 356). American Society of Civil Engineers.

Federal Emergency Management Agency. (2005). Improvement of nonlinear static seismic analysis procedures (FEMA 440). U.S. Department of Homeland Security.

Leiva Fuentes, N. G., Herrera, R. A., Massone, L. M., & Beltrán, J. F. (2024). Numerical modeling of beam plastic hinges in steel moment resisting frames including local buckling and stiffness/strength degradation. Structures, 69, Article 107260. https://doi.org/10.1016/j.istruc.2024.107260

Pratiwi, K. H., Purnomo, F. H., Nusantara, J. L. W., Majid, A. A., & Pramono, J. A. (2026). Kinerja seismik dan distribusi sendi plastis pada bangunan 20 lantai dengan dinding geser terputus terhadap beban gempa menggunakan analisis riwayat waktu nonlinear. Teras Jurnal: Jurnal Teknik Sipil, 16(2), 721–734. https://doi.org/10.29103/tj.v16i2.1438

Ramadhan, M. D. (2021). Perilaku Keruntuhan Struktur SRPM Baja Akibat Perbedaan Pemodelan Panel Zone (Studi Literatur). Jurnal Ilmiah Mahasiswa Teknik [JIMT], 1(2).

Safaei, S., Shamlu, M., & Vakili, A. (2022). Modeling methods and constitutive laws for nonlinear analysis of steel moment-resisting frames. Journal of Constructional Steel Research, 199, Article 107583. https://doi.org/10.1016/j.jcsr.2022.107583

Siahaan, H., & Prabowo, A. (2026). Efek variasi perilaku sendi plastis pada analisis pushover sistem RBKK tipe inverted-V. JMTS: Jurnal Mitra Teknik Sipil, 9(1), 107–122. https://doi.org/10.24912/jmts.v9i1.35823

Skiadopoulos, A., & Lignos, D. G. (2022). Seismic demands of steel moment resisting frames with inelastic beam-to-column web panel zones. Earthquake Engineering & Structural Dynamics, 51(7), 1591–1609. https://doi.org/10.1002/eqe.3629